Electrons and phonons in polymeric sulfur nitride

Michael Springborg
Nordisk Institut for Teoretisk Atomfysik (NORDITA), Blegdamsvej 17, DK-2100 København Ø, Denmark and Center for Materials Science, Los Alamos National Laboratory, Los Alamos, New Mexico 87545*
(Received 13 February 1989)

Results of first-principles calculations on a large number of geometries of a single, isolated, planar, periodic, infinite $(SN)_x$ chain are reported. The results are used in theoretically determining all four geometrical parameters, the single-particle energy bands, as well as frequencies and displacement patterns for frozen, zone-center, intrachain, in-plane phonons. The calculated values are compared with those derived from experiments and from other theoretical approaches. Finally, couplings between the electronic orbitals at the Fermi level and intrachain phonons are discussed.

I. INTRODUCTION

In 1910 Burt[1] reported the synthesis of "a new sulfide nitrogen." More than 40 years later the resulting compound was identified as a sulfur nitride polymer $(SN)_x$ (see, e.g., Ref. 2), and it was assumed[2] that each chain consisted of a zigzag arrangement of alternating sulfur and nitrogen atoms [Fig. 1(a)].

The discovery in 1973 by Walatka *et al.*[3] that the material remained metallic down to 4.2 K, which in 1975 was extended to 1.5 K by Greene *et al.*,[4] and the report by Greene *et al.*[5] later in 1975 that $(SN)_x$ undergoes a transition to a superconducting state at $T_c = 0.26 \pm 0.03$ K initiated a very large research activity in polymeric sulfur nitride (see, e.g., Refs. 6 and 7).

The major activity concentrated on a few key issues (see, e.g., Refs. 6 and 7). First of all, the material was ill-defined since it consisted of only partially parallel fibers each containing almost parallel macromolecules. This made it difficult experimentally to deduce a crystal structure as well as the geometry of a single polymer chain, and not until 1975 the correct structure of each macromolecule was determined for the first time by Boudelle[8] and later by Mikulski *et al.*[9] Both predict the structure of Fig. 1(b) to be that of a single polymer chain, but they differ in the relative arrangement of the chains. Although there were smaller differences in bond lengths and bond angles the former were essentially assumed for the zigzag structure of Fig. 1(a) (see, e.g., Ref. 10). The structure of Fig. 1(b) was able to explain how polymerization of planar almost square-shaped S_2N_2 molecules [Fig. 1(c)] lead to the $(SN)_x$ polymer.[11–13]

The other question that attracted much attention was why the polymer did not undergo a Peierls transition but remained metallic down to very low temperatures and became superconducting at even lower temperatures. Optical experiments and band-structure calculations (see, e.g., Refs. 7 and 14, and Sec. IV) were carried through in order to understand the nature of the electronic orbitals near the Fermi level. The band-structure calculations proposed one out of two reasons for the lacking Peierls distortion depending on the computational method. According to the first explanation two bands were crossing the Fermi level thus suppressing the Peierls transition, but it was later argued by Berlinsky[15] that this explanation could not hold, since in any true one-dimensional system with two bands crossing the Fermi level one could always find a total-energy lowering distortion that would open up gaps at the Fermi level. The other explanation (which now is believed to be the correct one; see, e.g., Ref. 16) proposed that interchain interactions — although relatively small — suppress the Peierls distortion.

Although the current interest in quasi-one-dimensional metals mostly concentrates on charge transfer salts and conjugated polymers presently (see, e.g., Ref. 17), there still remain a number of unsettled questions for polymeric sulfur nitride which call for a reconsideration of this

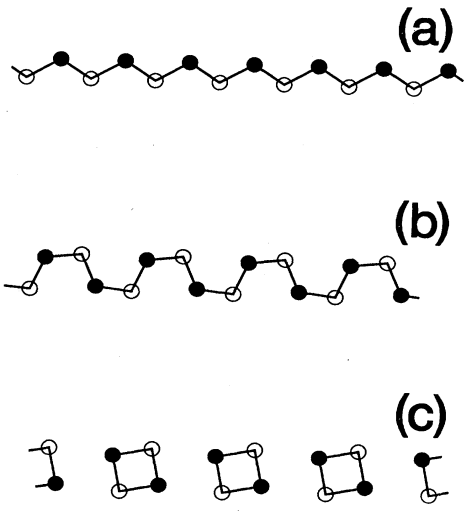

FIG. 1. (a) The earlier proposed form of a single poly(sulfur nitride) chain, (b) the correct structure, and (c) a part of a row of S_2N_2 molecules from the crystal structure of the latter. Comparing (c) and (b) it is clearly seen how polymerization of S_2N_2 molecules can lead to $(SN)_x$. The open (closed) circles represent nitrogen (sulfur) atoms.

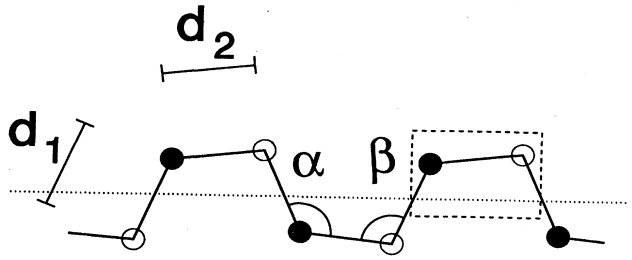

FIG. 2. The definition of the geometrical parameters for a single $(SN)_x$ chain of the form of Fig. 1(b). A zigzag symmetry is assumed and the dashed lines indicate a single unit cell, whereas the straight dotted line represents the polymer axis. The open and closed circles represent the nitrogen and sulfur atoms, respectively.

polymer. First of all, except for very few, all theoretical band-structure calculations considered only a single nuclear geometry, and there is accordingly no attempt to theoretically optimize the geometrical parameters. Hence, there has been no attempt from total-energy methods to determine the properties of the other important ingredient for superconductivity, namely the phonons. Furthermore, since the effective charge transfer from sulfur to nitrogen is large (around 0.4 electrons[13,18,19]) the lack of self-consistency in some of the theoretical investigations of the electronic structures might have crucial impacts on the results.

The purpose of this paper is to report results of self-consistent calculations on a large number of geometries of a single chain with the structure of Fig. 1(b). Assuming the chain to be planar and with a periodic zigzag structure the results are — among other applications — used in theoretically determining all four geometrical parameters (d_1, d_2, α, and β) shown in Fig. 2. The computational method has in detail been discussed elsewhere,[20,21] but a brief discussion is given in Sec. II. In Sec. III we report our optimized geometry and compare it with the experimentally derived ones. The band structures and electron densities are reported in Sec. IV, and the calculated frequencies and displacement patterns of some frozen zone-center phonons are given in Sec. V. Both in Sec. IV and in Sec. V comparisons with experimental and other theoretical values are carried through. A simple discussion of the couplings between the phonons and the electronic orbitals at the Fermi level, which are important for superconductivity, is presented in Sec. VI, and we conclude in Sec. VII. It should be pointed out that in the present approach interchain interactions are completely neglected. This will have some crucial consequences for the results, and we therefore briefly discuss their importance when appropriate.

II. METHOD OF COMPUTATION

We have applied our recently developed[20] self-consistent, first-principles, density-functional, full-potential, linear muffin-tin orbitals (LMTO) method for calculating the electronic structures of an infinite, periodic, isolated, helical chain. We assume the Born-Oppenheimer approximation valid and calculate thus the electronic distribution as determined by its own field and by the field generated by the fixed, nuclear point charges. There is accordingly no attempt to simultaneously solve the dynamical equations of the nuclei and the Schrödinger-like equations of the electrons,[22] which might be a drawback when analyzing the phonons and the electron-phonon couplings.

Within the Hohenberg-Kohn density-functional formalism[23] we make use of the local approximation to the exchange and correlation potential of von Barth and Hedin.[24] The resulting single-particle, Schrödinger-like Kohn-Sham equations[25] (in Ry atomic units)

$$[-\nabla^2+V(\mathbf{r})]\phi(\mathbf{r})=\varepsilon\cdot\phi(\mathbf{r}) \tag{1}$$

are solved by expanding the eigenfunctions $\phi(\mathbf{r})$ in (atom-centered) linear muffin-tin orbitals (LMTO's). A LMTO centered at $\mathbf{R}$ is defined as the numerical eigenfunction of (1) with $V(\mathbf{r})$ replaced by its spherically symmetric component inside a (muffin-tin) sphere at $\mathbf{R}$. On the sphere boundary it is matched continuously and once differentiably to a spherical Hankel function times a spherical harmonic, and inside any other muffin-tin sphere this product is augmented continuously and differentiably with the numerical functions of that sphere. The functions are thus eigenfunctions of a muffin-tin potential and as such good approximations to the exact solutions to (1), but it should be pointed out that with the LMTO basis functions we calculate the Hamilton matrices using the *full* potential as described elsewhere.[20,21]

We use a basis set consisting of two subsets, each containing s, p, and d functions on all sites and with one common decay constant of the Hankel functions for all atoms and (l,m) values. The two subsets differ in the decay constants. Nearly linearly dependent linear combinations are excluded through a canonical transformation.[26]

A single, isolated $(SN)_x$ chain such as that of Fig. 1(b) is assumed periodic and infinite. Its zigzag symmetry is thus a special case of the screw symmetry of a general helical polymer. For this latter we describe[20,21] the primitive screw symmetry operation as a combined translation of h and rotation of v. In a global coordinate system the position of the ith atom in the nth unit cell is

$$\begin{aligned} x &= r_i\cos(u_{ni}) , \\ y &= r_i\sin(u_{ni}) , \\ z &= (h/v)u_{ni}+z_i , \end{aligned} \tag{2}$$

with

$$u_{ni}=nv+\phi_i. \tag{3}$$

We will assume a single $(SN)_x$ polymer to be planar. This is a reasonable assumption since the mean deviation of the atomic positions from the common plane was reported by Boudelle[8] to be 0.32 a.u., whereas Mikulski *et al.*[9] and Heger *et al.*[27] did not notice any deviation from planarity at all. For later purposes we finally mention that the geometrical parameters of Fig. 2 correspond to

the following values of h, v, r_i, ϕ_i, and z_i:

$$h = d_2\cos[(\alpha-\beta)/2] - d_1\cos[(\alpha+\beta)/2] , \quad (4a)$$

$$v = \pi , \quad (4b)$$

$$r_N = \tfrac{1}{2}d_1\sin[(\alpha+\beta)/2] - \tfrac{1}{2}d_2\sin[(\alpha-\beta)/2] , \quad (4c)$$

$$r_S = \tfrac{1}{2}d_1\sin[(\alpha+\beta)/2] + \tfrac{1}{2}d_2\sin[(\alpha-\beta)/2] , \quad (4d)$$

$$\phi_N = \phi_S = 0 , \quad (4e)$$

$$z_N = 0 , \quad (4f)$$

$$z_S = d_2\cos[(\alpha-\beta)/2]. \quad (4g)$$

For the general helical polymer we make explicit use of the screw symmetry by forming Bloch waves from atom-centered basis functions defined in *local* right-handed coordinate systems with the z axis parallel to the screw axis and the x axis pointing away from it. For the planar zigzag $(SN)_x$ polymer of Fig. 2 local p_x and p_y functions of neighboring unit cells are thus antiparallel whereas the local p_z functions are parallel. Finally, the extra symmetry plane containing the nuclei makes it possible to separate the orbitals into π (formed by local p_y, d_{xy}, and d_{yz} functions) and σ orbitals.

III. STRUCTURE

By varying all four geometrical parameters we found the lowest total energy for $\alpha=122°$, $\beta=112°$, $d_1=3.30$ a.u., and $d_2=3.45$ a.u. (see Fig. 2). These values are to be compared with the electron diffraction results of Boudelle,[8] $\alpha=113.5°$, $\beta=111.5°$, $d_1=3.25$ a.u., and $d_2=2.99$ a.u.; with the x-ray diffraction results of Mikulski *et al.*,[9] $\alpha=120°$, $\beta=106°$, $d_1=3.08$ a.u., and $d_2=3.01$ a.u.; and with the neutron diffraction results of Heger *et al.*,[27] $\alpha=120°$, $\beta=107°$, and $d_1=d_2=3.00$ a.u.

It is noticed that whereas the bond angles are found in reasonable agreement with the experimental values, the bond lengths are significantly overestimated. Furthermore, the calculated relative order of d_1 and d_2 is reversed. In this context it should be added that we did not find any indication of (meta)stable structures with the experimental relative order of d_1 and d_2.

The reasons for the discrepancy can be manyfold. First of all, the interchain interactions, which are strong enough to suppress a Peierls transition, might also modify the bond lengths. Secondly, the density-functional formalism (or its local approximation) might overestimate the S—N bond lengths, and, finally, the present method might be responsible for the deviation. We will now discuss these possibilities.

Haddon *et al.*[28] have performed *ab initio* Hartree-Fock calculations on a number of finite molecules containing S—N bonds. Among those they considered were molecules formed by two or four SN units of the polymer terminated with single hydrogen atoms. For those they found S—N bond lengths ranging from 3.05 to 3.30 a.u., and $\alpha=101°-102°$ and $\beta=113°-117°$. Due to the termination it is difficult to relate their bond lengths to d_1 and d_2, but for the most middle bonds of the largest molecule a simple correspondence gives $d_1=3.13-3.22$ a.u. and $d_2=3.30$ a.u. Thus, their results show the same trend as ours except for a smaller overestimate of the bond lengths.

Earlier reports on sulfur and selenium helices[29,30] using the same method as in this report gave similar results: an overestimate in bond lengths, whereas bond angles and dihedral angles were in good agreement with experiments. Calculations on the S_3 molecule[31] using a related method predicted a slightly larger bond length compared with experimental values, whereas calculations on smaller selenium and sulfur clusters[32,33] using another density-functional method gave bond lengths with only small overestimates in bond lengths. Our calculations on the N_2 molecule[20] overestimated the bond length, as also was found with other density-functional methods, whereas the Hartree-Fock calculations underestimated the bond length (see, e.g., Ref. 20). This tendency was also found by Jones for the S_2 and S_3 molecules.[31] Finally, recent calculations[34] on As_2Se_3 (which due to the large Se content should be of relevance here) using another first-principles, density-functional method also predicted too large bond lengths.

In conclusion we believe therefore that the reversed order of d_1 and d_2 is due to the lacking interchain interactions, whereas these interactions as well as the density-functional formalism are responsible for the somewhat too large bond lengths.

This conclusion is also supported by our calculated total-energy differences between the optimized structure and the structure of Mikulski *et al.*[9] The difference, 1.40 eV per SN unit, is only slightly larger than the band splittings due to interchain interactions (see, e.g., Ref. 16).

These results indicate that d_1 is modified less than d_2 when the chains are allowed to interact, and we believe, therefore, that the most adequate viewpoint for discussing interactions between the electronic orbitals is to consider the SN units with the bonds of lengths d_1 as the building blocks. When the electronic orbitals of these units interact they will form weak interchain bonds and stronger intrachain bonds (the latter mainly being those with the lengths d_2).

We are only aware of three attempts to calculate structural properties of $(SN)_x$ using first-principles or *ab initio* methods. Kertész and co-workers[35] applied the *ab initio* Hartree-Fock method on three different geometries. They concluded that the structure of Fig. 1(b) is more stable than that of Fig. 1(a). A similar computational scheme was applied by Brédas,[36] who considered five geometries of undimerized and dimerized forms of Fig. 1(b). He concluded that the dimerization, in which a gap opens up at the Fermi level, is energetically favored. The same conclusion was obtained by Dovesi *et al.*,[37] who considered two structures of the form of Fig. 1(b) and also applied the *ab initio* Hartree-Fock approach. Due to the very limited number of geometries considered in

those reports it is not possible to extract detailed information on the structural parameters of $(SN)_x$.

IV. ELECTRONIC PROPERTIES

In Fig. 3 we depict the calculated band structures for the optimized geometry [Fig. 3(a)] and for the geometry of Mikulski *et al.*[9] [Fig. 3(b)]. As is common practice, we will neglect the formal lack of correspondence between the eigenvalues ε of (1) and electronic excitation values, since experience has shown this to be a good approximation.

In Fig. 3 we notice that the two sets of band structures are very similar except for a general narrowing when passing from Fig. 3(b) to Fig. 3(a). This is easily understood as due to the increased interatomic distances.

In order to facilitate the discussion of the band structures we show in Fig. 4 the electronic densities of each of the orbitals at the zone center and the zone edge for the bands of Fig. 3(b) (i.e., for the experimental geometry by Mikulski *et al.*,[9] but those for the optimized geometry show only minor deviations from those depicted).

The σ_1 and σ_2 bands [Figs. 4(a)–4(d)] are seen to be formed by local s and p orbitals and to be well localized to nearest-neighbor bonds. In contrast to this, the σ_3 and σ_4 bands [Figs. 4(e), 4(f), 4(l), and 4(m)] have significant next-nearest sulfur-nitrogen neighbor-pair interactions. Moreover, the σ_4 band at the zone edge [Fig. 4(m)] especially has important sulfur d components. Also the π bands are partially formed by sulfur d functions. Thus, the π_1 band at the zone center [Fig. 4(g)] is mainly a nitrogen p function, but the sulfur d components cause both the elongation of the electron density towards the sulfur nuclei as well as the nodal curves close to the sulfur nuclei. The π_1 band at the zone edge [Fig. 4(h)] is mainly p_y functions on both sulfur and nitrogen, whereas the π_2 band at the zone center [Fig. 4(i)] has dominating sulfur p components, which become mixed with increasing amounts of sulfur d functions as the zone boundary is approached [cf. Fig. 4(j) for the orbital at the Fermi level and Fig. 4(k) for that at the zone edge]. Thus, sulfur d functions are important in this approach as they have also proven to be in the *ab initio* Hartree-Fock approaches of Haddon *et al.*[28] on finite molecules and of Dovesi *et al.*[37] on a single $(SN)_x$ chain.

We will now compare our results with those obtained with other theoretical methods. In doing this we will not consider the early works which solely considered the incorrect geometry of Fig. 1(a) (for a review including those, see, e.g., Ref. 14). We will furthermore only examine some few key quantities, these being the total valence-band width W_v, the width of the occupied part of the uppermost π valence band W_π, the ionization potential V_{IP} (which is undefined for the methods considering a three-dimensional, infinite solid), the density of states at the Fermi level $D(\varepsilon_F)$, and the effective mass at the Fermi level m^*/m_e. The first quantity will give a general measure of the accuracy of the applied methods, and the other quantities are important for the conducting and superconducting properties of the materials. In Table I we have collected our values together with those of other

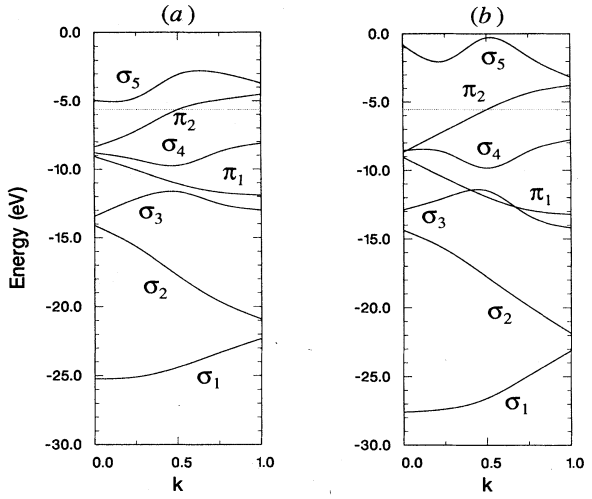

FIG. 3. The valence and the lowest conduction bands for a single $(SN)_x$ chain for the optimized (experimental) geometry in (a) [(b)]. The Fermi level is indicated as the dotted line.

theoretical approaches and of some experiments. In evaluating the data of Table I some remarks should be made.

We report two sets of values for the present approach; one for the experimental geometry and one for the optimized one. The effective mass depends on the second derivative of the single-particle energies and is accordingly connected with some uncertainty.

The first two reports (Refs. 38–40) are included as examples of those finding both σ and π bands crossing the Fermi level. This is in contrast to most later findings and we have therefore only included those two as representative.

Rajan and Falicov[38] considered both the zigzag structure of Fig. 1(a) as well as the planar structure of Fig. 1(b), and for the latter they used bond angles and bond lengths both as determined by Boudelle[8] and as determined by Mikulski *et al.*[9] Molecular orbitals from self-consistent *ab initio* calculations on a single SN molecule were transferred to a single $(SN)_x$ chain and a non-self-consistent calculation giving the band structures was carried through. In contrast to this the calculations of Kamimura and co-workers[39,40] were pure semiempirical tight-binding calculations.

The rest of the reports to be mentioned here found only one (π) band to cross the Fermi level. Among the semiempirical calculations are extended Hückel calculations by Bright and Soven[41] and by Friesen *et al.*[42] on crystalline SN and by Salahub and Messmer[43,44] on different numbers of interacting chains. Furthermore, the semiempirical CNDO (complete neglect of differential overlaps) method was applied by Suhai and Kertész[45] on one chain and by Tanaka and co-workers[46] on two interacting chains. As based upon the Hartree-Fock approximation it overestimates bandwidths. Semiempirical pseudopotential calculations on three-dimensional SN were carried through by Schlüter *et al.*[47,48] The last semiempirical cal-

culations we will mention here are the VEH calculations (valence effective Hamiltonian) by Brédas[49] on a single chain. The method is designed to reproduce *ab initio* Hartree-Fock results, and the widths are accordingly too large.

A number of *ab initio* Hartree-Fock calculations on a single isolated chain have been reported. Among those are calculations by Kertész *et al.*[35] and by Suhai and Ladik.[50] Finally, Dovesi and co-workers[16,37] have applied the *ab initio* Hartree-Fock method first on a single chain (Ref. 36) and later on two and more interacting chains (Ref. 16). Their detailed discussion of the interchain interactions demonstrates that these are of minor importance for charge densities and bond populations but have appreciable influence on the electronic properties. It is important to keep this in mind when comparing results of calculations on one chain with those on more chains.

Also a number of density-functional calculations have been reported. These include the non-self-consistent OPW (orthogonalized-plane-waves) calculations by

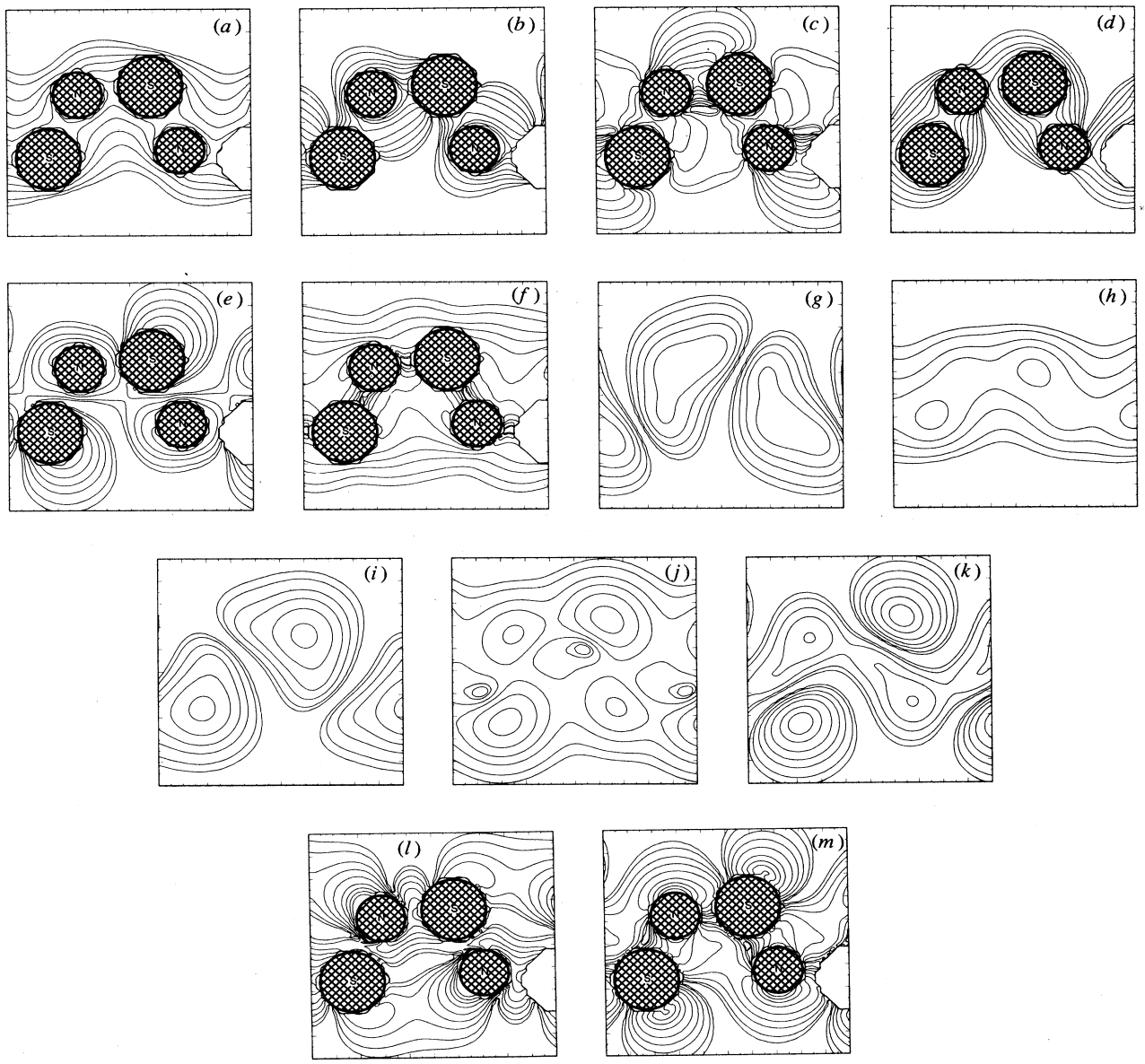

FIG. 4. Contour curves of the electron densities outside the interior of the muffin-tin spheres for some of the orbitals for a single chain with the experimental geometry. Shown are those of the σ_1 [(a),(b)], the σ_2 [(c),(d)], the σ_3 [(e),(f)], the π_1 [(g),(h)], the π_2 [(i),(k)], and the σ_4 [(l),(m)] orbitals at the zone center [(a),(c),(e),(g),(i),(l)] and zone edge [(b),(d),(f),(h),(k),(m)] together with those of the π_2 orbital at the Fermi level (j). Those of the σ orbitals are shown in the plane of the nuclei where the largest (smallest) spheres are those of sulfur (nitrogen), and the densities of the π orbitals are shown in the same plane but lifted 1.75 a.u. above the plane of the nuclei. Contour values are 0.10, 0.08, 0.06, 0.04, 0.02, 0.01, 0.005, 0.002, and 0.001 a.u., and the size of the planes is 10×10 a.u.

Rudge, Grant, and co-workers.[51,52] The experimental three-dimensional geometries of Boudelle[8] and of Mikulski *et al.*[9] were considered and the results differed only little for the two structures.

In contrast to these calculations those on both a single $(SN)_x$ chain and on three-dimensional crystalline SN by Ching *et al.*[53] were self-consistent. Another difference was the use of an atom-centered basis set in the calculations by Ching *et al.* It is surprising that they found the total valence-band width to be smaller for the three-dimensional structure than for the single chain.

Both Ching *et al.*[53] and Batra and co-workers[54,55] have compared crystalline SN and crystalline S_2N_2 using first-principles, density-functional methods, but the calculations by Batra *et al.*[54] were not self-consistent. Batra and co-workers examined the effects of including sulfur *d* functions in the basis set (these were omitted in most of the works mentioned above) and found them to be small in contrast to our findings and to those of Haddon *et al.*[28]

Mihich[56] applied the self-consistent, density-functional, so-called intersecting spheres model on a single chain of polymeric sulfur nitride. He found only small differences between the values for the structure of Boudelle[8] and for that of Mikulski *et al.*[9]

The last theoretical work on the band structures of $(SN)_x$ we will mention is the self-consistent, first-principles, density-functional calculations by Oshiyama and Kamimura[57] on the crystalline material. They used a basis set of numerical atom-centered functions.

In comparing our values with those above we notice more features. First of all, the calculations based on the Hartree-Fock approximation (i.e., the CNDO, VEH, and *ab initio* Hartree-Fock calculations) yield significantly larger bandwidths than the other calculations. Our value for W_v for the experimental structure is slightly smaller than that of the other non-Hartree-Fock calculations. On the other hand, the values of W_π show only little systematic trends and for this we find a somewhat larger value than that of most other non-Hartree-Fock calculations. We propose that the sulfur *d* functions explain the

TABLE I. Various band-structure properties for $(SN)_x$ as obtained with theoretical (present, Refs. 16, 35, and 38–54) and experimental (Refs. 4 and 66–69) methods. Listed is the total valence-band width (W_v, in eV), the width of the occupied part of the π_2 band (W_π, in eV), the ionization potential (V_{IP}, in eV), the density of states at the Fermi level [$D(\varepsilon_F)$, in states/(spin eV molecule) with one molecule being one SN unit], and the effective mass at the Fermi level (m^*/m_e). We report values both for the experimental geometry (labeled "expt.") and the optimized geometry ("optim."). The semiempirical theoretical methods include tight-binding (TB), extended Hückel (EH), pseudopotential (PP), complete neglect of differential overlaps (CNDO), and valence-effective-Hamiltonian (VEH) methods. HF labels *ab initio* Hartree-Fock calculations, and first-principles calculations using orthogonalized plane waves (OPW), atom-centered basis functions (LCAO), and the intersecting-spheres method (IS) are listed. The calculations labeled non-SCF were not self-consistent. The experimental results have been obtained from x-ray photoelectron spectroscopy (XPS), and specific-heat (SH) and optical reflectivity (OR) experiments. The reader is referred to the text for further details.

Ref.	W_v	W_π	V_{IP}	$D(\varepsilon_F)$	m^*/m_e	Comment
			Theory			
Present work	22.0	3.1	5.6	0.18	1–3	expt.
Present work	19.6	2.7	5.5	0.22	1–3	optim.
38	~19		~12			non-SCF LCAO
39,40			~9			TB
41		1.4				EH
42		0.9		0.16		EH
43,44	22	~2.3	~7.7			EH
45	~32	6.3	~5.6			CNDO
46	34	5	6			CNDO
47,48	22	2		0.12		PP
49	28	2.6	~3.4	0.14		VEH
16	~32.5	6.5		0.085		HF
35	~34	5.6	~1.5	0.1	2.2	HF
50		2.0	~7.8	0.14	1.7	HF
51,52	~27.5	~2.5				non-SCF OPW
53	26	~1.5		0.01		LCAO
54	24	1.7				non-SCF LCAO
56	24	~2.3	6	0.23		IS
57	23	~1.6		0.14		LCAO
			Experiments			
58	24.4					XPS
4				0.18		SH
66				0.14		SH
67					5.2	OR
68					2	OR
69					2.5	OR

differences. These are less important for the lowest valence bands, as the discussion of the electron densities showed, but are important for the π_2 band. Exclusion of the sulfur d functions will give a poorer description of the π_2 band and thus a too narrow band. Inclusion of them will move the occupied part of the π_2 band to lower energies, whereas the σ_1 band is only little affected. Thus, the total valence-band width will be decreased upon inclusion of sulfur d functions.

We find the effective mass and the density of states at the Fermi level in good agreement with the findings of other theoretical approaches although the theoretical values of the latter vary much.

The interchain interactions make a comparison with experimental values of the quantities close to the Fermi level difficult. However, with this in mind we will now turn to a discussion of the experimental results on $(SN)_x$.

X-ray photoelectron spectroscopy (XPS) on $(SN)_x$ has been performed by Ley[58] and by Mengel *et al.*,[59] and ultraviolet photoemission spectroscopy (UPS) has been carried out by Koch and Grobman.[60] Although matrix-element effects will modify the relative heights of the peaks when comparing calculated density-of-states curves and XPS and UPS data,[55] the positions of the peaks will not be changed, and we will here simply relate the flat parts of the bands in Fig. 3(b) for the experimental geometry with the peaks in the XPS and UPS spectra. Due to different cross sections XPS gives information mainly on the s-like orbitals whereas UPS has its largest amplitudes for p-like orbitals.

Ley[58] noticed four peaks in his XPS spectra. These were placed at 21.0, 15.2, 7.4, and 3.6 eV, respectively, below the Fermi level, ε_F. The first peak agrees fairly well with the position of the bottom of the σ_1 band, which we calculate to be 22.0 eV below ε_F. The third and fourth peaks might be related to the σ_3 and σ_4 bands; we find these to be at 5.9–8.6 eV and 2.2–4.3 eV below ε_F, respectively. For the second peak (at 15.2 eV) we do not find any direct counterpart. It is, however, low and broad and could therefore be related to the σ_1 and σ_2 bands at the zone edges. Finally, the total valence-band width was reported by Ley to be 24.4 eV. This larger width and a shoulder at 0.7 eV below ε_F we believe to be due to interchain couplings.

The XPS data by Mengel *et al.*[59] differ only a little from those of Ley,[58] except that the second peak is split into two. This is consistent with our interpretation of the origin of this peak.

In their UPS measurements Koch and Grobman[60] considered both films and single crystals. They have listed a number of peaks in the region 0.2–16.2 eV below the Fermi level. Two peaks at 1.2 and 2.5 eV might be related to interchain couplings and to the top of the σ_4 band, respectively. Their four peaks in the region 4.9–10.2 eV we will relate to the π_1 and σ_3 bands, and finally, we believe the σ_2 and σ_1 bands at the zone edge to be responsible for their peaks at 14.3 and 16.1 eV, respectively.

In total we find the agreement with the XPS and UPS spectra and our band structures for the experimental geometry good.

Valence- to conduction-band transitions as measured by synchrotron-radiation-reflectivity experiments have been discussed by Bordas *et al.*[61] and by Mitani *et al.*[62–64] As is well known, calculations based on the density-functional formalism usually predict conduction states lying too close to the Fermi level, and a comparison between our band structures and the experimental dielectric constant ϵ_2 will be complicated by this "band-gap" problem. We will therefore only compare here with one of the more recent and detailed experimental studies on $(SN)_x$, namely, Ref. 64 by Mitani and co-workers. It should be noticed that when comparing we are to use a translational symmetry of the polymer, and the unit cell is thus to be doubled and the bands of Fig. 3 to be folded about $k = 0.5$. However, in the discussion below we will refer to the unfolded band structures of Fig. 3.

Mitani *et al.*[64] reported seven peaks at 2.7, 4.1, 4.9, 5.8, 7.5, 11, and 15 eV, respectively. The first they have ascribed the $\pi_2(k=0)\rightarrow\pi_2(k=1)$ transition and is thus considerably smaller than our calculated width of 4.9 eV. The peaks at 4.1 and 4.9 eV they ascribed $\pi_2(k=0)\rightarrow\sigma_5(k=1)$ transitions, which we find to be 5.4 eV, and the peak at 5.8 eV they believed to be due to $\sigma_4\rightarrow\sigma_5$ and $\sigma_4\rightarrow\pi_2(k=1)$ transitions, which is in reasonable agreement with our findings. Finally, they ascribe the peaks at 7.5 and 11 eV partly $\sigma_4\rightarrow\sigma_5$ (7.5 eV), $\sigma_3\rightarrow\sigma_5$ (11 eV), and $\pi_1\rightarrow\pi_2$ (11 eV) transitions. These values agree reasonably with those we find: 7–8 eV, 9–12 eV, and 9.5 eV, respectively.

We should mention that interchain couplings, which are fairly strong for the orbitals close to the Fermi level, complicate the comparison. But we believe all transitions at 2.7, 4.1, and 4.9 eV to be $\pi_2\rightarrow\pi_2$ transitions. Furthermore, we would assign the $\pi_2\rightarrow\sigma_5$ transition the peak at 5.8 eV, when remembering the "band-gap" problem. And, finally, due to interchain couplings we believe the $\sigma_3\rightarrow\sigma_5$ transition to contribute to both peaks at 7.5 and 11 eV. Taking this reassignment into account we find the agreement fair.

Electron-energy-loss spectroscopy (EELS) makes it possible not only to measure vertical transitions but also transitions with nonzero momentum transfer. Among others, Stolz *et al.*[65] have performed EELS experiments on polymeric sulfur nitride. For zero momentum transfer their data resemble the synchrotron data of Mitani *et al.*[64] with peaks at 1.7, 4.4, 6.2, 8.2, 12.0, 17.0, and 22.3 eV, and an interpretation like that of the synchrotron data should be possible.

A value of the density of states at the Fermi energy, $D(\varepsilon_F)$, has been derived by Greene *et al.*[4] from specific-heat experiments. They obtained $D(\varepsilon_F)=0.18$ states/(eV spin molecule), whereas Harper *et al.*[66] from similar experiments derived $D(\varepsilon_F)=0.14$ states/(eV spin molecule). These values agree well with ours.

There seems to be greater uncertainty about the effective mass at the Fermi level, m^*/m_e. Bright *et al.*[67] have reported a value of 5.2 for films, whereas Grant *et al.*[68] estimated it to be 2 for a crystalline material, and Gutman *et al.*[69] found it to be 2.5 also for a crystal. Our values seem to be in best agreement with those derived

for crystalline materials, but also here interchain couplings make a comparison difficult.

V. PHONONS

Close to the optimized geometry we expand the total energy to second order in bond lengths and bond angles as

$$E \simeq \varepsilon_{\rm la} = e_0 + e_1 d_1 + e_2 d_2 + e_\alpha \alpha + e_\beta \beta + e_{11} d_1^2 + e_{22} d_2^2 + e_{\alpha\alpha} \alpha^2 + e_{\beta\beta} \beta^2 + e_{12} d_1 d_2 + e_{1\alpha} d_1 \alpha + e_{1\beta} d_1 \beta + e_{2\alpha} d_2 \alpha + e_{2\beta} d_2 \beta + e_{\alpha\beta} \alpha\beta . \quad (5)$$

However, for our purpose it is more convenient to use the parameters of Eq. (4), and by retaining a harmonic approximation and using Eq. (4) we thus arrive at

$$E \simeq \varepsilon_{\rm hp} = e_0 + e_h h + e_{r_{\rm N}} r_{\rm N} + e_{r_{\rm S}} r_{\rm S} + e_{z_{\rm S}} z_{\rm S} + e_{hh} h^2 + e_{r_{\rm N} r_{\rm N}} r_{\rm N}^2 + e_{r_{\rm S} r_{\rm S}} r_{\rm S}^2 + e_{z_{\rm S} z_{\rm S}} z_{\rm S}^2 + e_{h r_{\rm N}} h r_{\rm N} + e_{h r_{\rm S}} h r_{\rm S} + e_{h z_{\rm S}} h z_{\rm S} + e_{r_{\rm N} r_{\rm S}} r_{\rm N} r_{\rm S} + e_{r_{\rm N} z_{\rm S}} r_{\rm N} z_{\rm S} + e_{r_{\rm S} z_{\rm S}} r_{\rm S} z_{\rm S} . \quad (6)$$

We calculated the total energy for the 81 geometries defined by $d_1 = 3.25$, 3.30, and 3.35 a.u., $d_2 = 3.40$, 3.45, and 3.50 a.u., $\alpha = 120°$, 122°, and 124°, and $\beta = 110°$, 112°, and 114°. The minimum was found for the "middle" calculation, i.e., $d_1 = 3.30$ a.u., $d_2 = 3.45$ a.u., $\alpha = 122°$, and $\beta = 112°$, as already indicated by the results reported in Sec. III.

Least-squares fitting the 81 total energies with (5) or (6) turned out to be very difficult due to almost linear dependencies of the fitting functions (over-completeness), and also using the so-called singular-value decomposition technique (see, e.g., Ref. 70) resulted often in fits predicting no global total-energy minimum. We therefore, first of all, restricted the number of parameters by requiring $\varepsilon_{\rm la}$ or $\varepsilon_{\rm hp}$ to reproduce the above-mentioned geometry to be that of the lowest total energy.

Wendel[71] has used a model of the form (5) extended with interchain interactions in order to reproduce experimentally derived phonon frequencies. He only kept $e_{11} = e_{22}$ and $e_{\alpha\alpha} = e_{\beta\beta}$ nonzero, but included intrachain interactions between next-nearest nitrogen-sulfur pairs. Since we explicitly make use of the zigzag symmetry and furthermore only consider zone-center displacements, we cannot distinguish between the last interaction and that of e_{22}. Keeping all constants of (5) zero except for e_{11}, e_{22}, $e_{\alpha\alpha}$, and $e_{\beta\beta}$ we find $e_{11} = 7.90$ eV/bohr^2, $e_{22} = 6.26$ eV/bohr^2, $e_{\alpha\alpha} = 0.0080$ eV/deg^2, and $e_{\beta\beta} = 0.0055$ eV/deg^2. Wendel reported $e_{11} = e_{22} = 1.93 \times 10^5$ dyn/cm $= 3.37$ eV/bohr^2, which is only half the values of ours. He reported furthermore values of $e_{\alpha\alpha} = e_{\beta\beta}$ of almost 2 orders of magnitude smaller than ours. However, part of the discrepancy can be explained as due to his inclusion of next-nearest-neighbor interactions. Moreover, the lacking interchain interactions in the present approach will influence the results. These interactions might weaken the intrachain bonds and thus soften the intrachain phonons.

It turned out that in order to avoid over-completeness the best strategy in fitting our first-principles total energies was to restrict the fit (6) to

$$\varepsilon_{\rm hp} = e_0 + e_{hh} (\Delta h)^2 + e_{r_{\rm N} r_{\rm N}} (\Delta r_{\rm N})^2 + e_{r_{\rm S} r_{\rm S}} (\Delta r_{\rm S})^2 + e_{z_{\rm S} z_{\rm S}} (\Delta z_{\rm S})^2 + e_{r_{\rm N} r_{\rm S}} (\Delta r_{\rm N})(\Delta r_{\rm S}) , \quad (7)$$

where all lengths are relative to the values of the optimal geometry. Here, e_{hh} is related to the compressibility of the material along the chains.

When the parameters had been obtained we replaced $\Delta z_{\rm S}$ with $\Delta z_{\rm S} - \Delta z_{\rm N}$ and the phonon frequencies could be calculated as the eigenvalues of $(\partial^2 \varepsilon_{\rm hp} / \partial x_i \partial x_j)/(M_i M_j)^{1/2}$, with $x_i = \Delta r_N$, Δz_N, Δr_S, and Δz_S for $i = 1$, 2, 3, and 4, respectively, and $M_i = M_N$, $M_{\rm N}$, $M_{\rm S}$, and $M_{\rm S}$ for $i = 1$, 2, 3, and 4, respectively. Here, $M_{\rm N}$ ($M_{\rm S}$) is the atomic mass of nitrogen (sulfur).

Except for the trivial zero-frequency mode we found three modes at roughly 500, 900, and 1200–1500 cm^{-1}, where the variations in the last frequency were related to different fitting strategies. Unfortunately, we are not able to choose a single set of frequencies as the optimal one.

The modes of the lowest and highest frequency correspond to antisymmetric and symmetric oscillations in $\Delta r_{\rm N}$ and $\Delta r_{\rm S}$, respectively, with the amplitude on the nitrogen atoms being largest for the highest-frequency mode, and smallest for the low-frequency mode.

There exist some reported experimental phonon frequencies for $(SN)_x$. Temkin and Fitchen[72] have reported Raman spectra on the compound. They observed features at 454, 621, 658, and 782 cm^{-1}. The force model by Wendel gave — using a translational symmetry — zone-center high-frequency modes at 660, 775, 895, and 985 cm^{-1}. Raman scattering experiments on pure and brominated $(SN)_x$ by Temkin and Street[73] gave high-frequency modes at 456, 658, and 786 cm^{-1} in excellent agreement with those of Temkin and Fitchen. One of the most detailed investigations of the phonon spectrum of poly(sulfur nitride) was undertaken by Macklin *et al.*[74] using infrared spectroscopy. Of relevance to the present work are their modes at 1001 and 500 cm^{-1}, which they ascribe displacement patterns analogous to those we find for the highest and next-highest frequencies. A mode at 629 cm^{-1} might be similar to that of our lowest frequency.

In total we notice significant differences between our phonon frequencies and the experimentally determined ones. The largest difference seems to be a general shift towards higher frequencies. This is consistent with our finding of larger spring constants compared with those of Wendel.[71] Since interchain couplings have some importance these will of course lead to different results when considering a three-dimensional structure instead of the quasi-one-dimensional structure considered here. Also our finding of an optimized structure with somewhat different bond lengths than the experimental structure

(again partly due to the lack of interchain couplings) modifies the results.

Despite the discrepancies between the calculated and measured frequencies we believe the general trends in the frequencies and displacement patterns of these modes are obtained. We will therefore use these in the next section in a semiquantitative discussion of some electron-phonon couplings. Due to the very limited number of phonons considered here we cannot estimate the electron-phonon coupling constants.

VI. ELECTRON-PHONON COUPLINGS

The essential part of the electron-phonon couplings important for the superconductivity is a description of how the orbitals at the Fermi level vary under the influence of a phonon (see, e.g., Refs. 75–77).

For a single $(SN)_x$ chain we notice three important features. First of all, the Fermi surface reduces to two single points ($k = \pm 0.5$ in the units of Fig. 3), secondly, only one band crosses the Fermi level, and, thirdly, since the chain is finite in two dimensions the absolute value of the Fermi energy has a meaning. Thus, a simple measure of the electron-phonon couplings for this system is the shift of the Fermi energy when a phonon is excited in a single chain. This is the approach we will use for the three frozen, zone-center, intrachain, in-plane phonons calculated in the preceding section.

Assuming the phonons to have an amplitude of 0.05 a.u. we estimate the Fermi energy to vary roughly 0.06, 0.04, and 0.03 eV for the phonon with the lowest, middle, and highest frequency, respectively. These numbers are small and should be taken with much caution, although we believe them to reproduce the general physics, as we shall argue below.

From Fig. 4 we notice that there are important electronic interactions between those next-nearest sulfur-nitrogen pairs, which in the S_2N_2 compound are connected with bonds [see Figs. 1(b) and 1(c)]. Therefore, phonons involving displacements of the atoms perpendicular to the chains will mainly only affect one type of bond; namely those with the lengths d_1 (see Fig. 2), and will accordingly be the softest phonons. The phonons with displacements parallel with the polymer axis change both the bond lengths d_2 and the weaker next-nearest-neighbor bonds and will therefore have higher frequencies.

On the other hand, Fig. 4(j) clearly demonstrates that the orbital at the Fermi level has the largest components on the sulfur atoms. Therefore, the phonons displacing the sulfur atoms most will lead to the largest changes in the Fermi energy.

Finally, in an improved more realistic approach the phonons would have amplitudes that are smallest (largest) for those with the largest (smallest) frequencies. To lowest order in the amplitude this would not change the trend but result in even larger differences in the Fermi-level shifts.

In total we therefore believe that the softest of the frozen, zone-center, in-plane, intrachain phonons is the important one for superconductivity. It should be added that this result agrees qualitatively with our preliminary result reported earlier.[21] In that report we considered the changes in the total energy and in the Fermi energy when starting from the experimental geometry of Boudelle[8] moving either all sulfur atoms or all nitrogen atoms in unison either perpendicular or parallel to the polymer axis. Also there we found the smallest changes in the total energy and the largest changes in the Fermi energy when moving the sulfur atoms perpendicular to the polymer axis.

VII. CONCLUSIONS

We have applied the self-consistent, first-principles, density-functional, full-potential, LMTO method[20] for helical polymers on a large number of geometries of a single planar poly(sulfur nitride) chain. To our knowledge this is the only detailed investigation of the structural properties of $(SN)_x$ using a parameter-free method. The main results are as follows.

From the calculations we determined the structure with the lowest total energy, when restricting ourselves to structures with the geometry of Fig. 2. The bond angles were found in good agreement with the experimental data, but the bond lengths were somewhat overestimated, and, moreover, the relative order of the lengths of the bonds almost parallel to the polymer axis and of those intersecting this axis was reversed. We argued the latter to be largely due to the single-chain approximation used here.

The single-particle energy bands were found to be very similar for the experimental and the optimized geometry except for a general narrowing of those of the latter. As compared with results of Hartree-Fock calculations, our results as well as most other density-functional results are in significantly better agreement with the experimental results.

In particular for the half-filled π_2 band we found sulfur d functions to be important. These functions led to a larger width of this band compared with results of many other calculations on $(SN)_x$.

The comparison of experimental XPS and UPS data with our valence bands for the experimental geometry gave good agreement, and band-to-band transitions as measured by synchrotron radiation experiments and by EELS experiments could also be interpreted in good agreement with the present results.

The density of states at the Fermi level and the effective mass at the Fermi level were found in reasonable agreement with the experimental values, although these quantities are sensitive to interchain interactions.

We found, in general, the frequencies of frozen zone-center phonons to be larger than the experimentally derived ones. We believe the general explanation for this to be the lack of interchain couplings in our calculations — these also leading to a different optimized structure.

Finally, we examined the way the Fermi energy changed when the various frozen, zone-center, in-plane, intrachain phonons were excited, thereby obtaining an es-

timate of the electron-phonon couplings, which are important for superconductivity. It turned out that the softest of these phonons — involving the largest displacements of the sulfur atoms perpendicular to the polymer axis — coupled strongest to the electronic orbitals at the Fermi level.

ACKNOWLEDGMENTS

The author acknowledges a careful reading of the manuscript by Dr. Alan Luther. Furthermore, this work was supported by the Danish Natural Science Research Council.

---

*Permanent address.

[1]F. P. Burt, J. Chem. Soc. London **97**, 1171 (1910).

[2]M. Goehring, Quart. Rev. Chem. Soc. **10**, 437 (1956).

[3]V. V. Walatka, Jr., M. M. Labes, and J. H. Perlstein, Phys. Rev. Lett. **31**, 1139 (1973).

[4]R. L. Greene, P. M. Grant, and G. B. Street, Phys. Rev. Lett. **34**, 89 (1975).

[5]R. L. Greene, G. B. Street, and L. J. Suter, Phys. Rev. Lett. **34**, 577 (1975).

[6]R. L. Greene and G. B. Street, in *Chemistry and Physics of One-Dimensional Metals,* edited by H. J. Keller (Plenum, New York, 1977).

[7]M. M. Labes, P. Love, and L. F. Nichols, Chem. Rev. **79**, 1 (1979).

[8]M. Boudelle, Cryst. Struct. Commun. **4**, 9 (1975).

[9]C. M. Mikulski, P. J. Russo, M. S. Saran, A. G. MacDiarmid, A. F. Garito, and A. J. Heeger, J. Am. Chem. Soc. **97**, 6358 (1975).

[10]M. Boudelle and P. Michel, Acta Crystallogr., Sect. A **28**, S199 (1972).

[11]M. J. Cohen, A. F. Garito, A. J. Heeger, A. G. MacDiarmid, C. M. Mikulski, M. S. Saran, and J. Kleppinger, J. Am. Chem. Soc. **98**, 3844 (1976).

[12]R. H. Baughman, R. R. Chance, and M. J. Cohen, J. Chem. Phys. **64**, 1869 (1976).

[13]D. R. Salahub and R. P. Messmer, J. Chem. Phys. **64**, 2039 (1976).

[14]J. L. Brédas, Ann. Soc. Sci. Bruxelles **94**, 83 (1980).

[15]A. J. Berlinsky, J. Phys. C **9**, L283 (1976).

[16]M. Causá, R. Dovesi, C. Pisani, C. Roetti, and V. R. Saunders, J. Chem. Phys. **88**, 3196 (1988).

[17]Proceedings of the International Conference on Science and Technology of Synthetic Metals 1988, Santa Fe, New Mexico [Synth. Metals **27-29** (1988-1989)].

[18]W. R. Salaneck, J. W.-p. Lin, and A. J. Epstein, Phys. Rev. B **13**, 5574 (1976).

[19]R. Larsson, J. Electron Spectrosc. Relat. Phenom. **24**, 37 (1981).

[20]M. Springborg and O. K. Andersen, J. Chem. Phys. **87**, 7125 (1987).

[21]M. Springborg, J. Chim. Phys. **86**, 715 (1989).

[22]R. Car and M. Parrinello, Phys. Rev. Lett. **55**, 2471 (1985).

[23]P. Hohenberg and W. Kohn, Phys. Rev. **136**, B864 (1964).

[24]U. von Barth and L. Hedin, J. Phys. C **5**, 1629 (1972).

[25]W. Kohn and L. J. Sham, Phys. Rev. **140**, A1133 (1965).

[26]P.-O. Löwdin, Adv. Quant. Chem. **5**, 185 (1970).

[27]G. Heger, S. Klein, L. Pintschovius, and H. Kahlert, J. Solid State Chem. **23**, 341 (1978).

[28]R. C. Haddon, S. R. Wasserman, F. Wudl, and G. R. J. Williams, J. Am. Chem. Soc. **102**, 6687 (1980).

[29]M. Springborg and R. O. Jones, Phys. Rev. Lett. **57**, 1145 (1986).

[30]M. Springborg and R. O. Jones, J. Chem. Phys. **88**, 2652 (1988).

[31]R. O. Jones, J. Chem. Phys. **84**, 318 (1986).

[32]D. Hohl, R. O. Jones, R. Car, and M. Parrinello, Chem. Phys. Lett. **139**, 540 (1987).

[33]D. Hohl, R. O. Jones, R. Car, and M. Parrinello, J. Chem. Phys. **89**, 6823 (1988).

[34]E. Tarnow, M. C. Payne, and J. D. Joannopoulos, Phys. Rev. Lett. **61**, 1772 (1988).

[35]M. Kertész, J. Koller, and A. Ažman, Phys. Status Solidi B **77**, K157 (1976).

[36]J. L. Brédas, J. Phys. C **15**, 3473 (1982).

[37]R. Dovesi, C. Pisani, C. Roetti, and V. R. Saunders, J. Chem. Phys. **81**, 2839 (1984).

[38]V. T. Rajan and L. M. Falicov, Phys. Rev. B **12**, 1240 (1975).

[39]H. Kamimura, A. J. Grant, F. Levy, and A. D. Yoffe, Solid State Commun. **17**, 49 (1975).

[40]H. Kamimura, A. M. Glazer, A. J. Grant, Y. Natsume, M. Schreiber, and A. D. Yoffe, J. Phys. C **9**, 291 (1976).

[41]A. A. Bright and P. Soven, Solid State Commun. **18**, 317 (1976).

[42]W. I. Friesen, D. B. Litvin, and B. Bergersen, Phys. Status Solidi B **85**, 715 (1978).

[43]R. P. Messmer and D. R. Salahub, Chem. Phys. Lett. **41**, 73 (1976).

[44]D. R. Salahub and R. P. Messmer, Phys. Rev. B **14**, 2592 (1976).

[45]S. Suhai and M. Kertész, J. Phys. C **9**, L347 (1976).

[46]K. Tanaka, T. Yamabe, K. Fukui, A. Imamura, and H. Kato, Chem. Phys. Lett. **53**, 452 (1978).

[47]M. Schlüter, J. R. Chelikowsky, and M. L. Cohen, Phys. Rev. Lett. **35**, 869 (1975), **36**, 452(E) (1976).

[48]J. R. Chelikowsky, M. Schlüter, and M. L. Cohen, Phys. Status Solidi B **82**, 357 (1977).

[49]J. L. Brédas, Chem. Phys. Lett. **115**, 119 (1985).

[50]S. Suhai and J. Ladik, Solid State Commun. **22**, 227 (1977).

[51]W. E. Rudge and P. M. Grant, Phys. Rev. Lett. **35**, 1799 (1975).

[52]P. M. Grant, R. L. Greene, W. D. Gill, W. E. Rudge, and G. B. Street, Mol. Cryst. Liq. Cryst. **32**, 171 (1976).

[53]W. Y. Ching, J. G. Harrison, and C. C. Lin, Phys. Rev. B **15**, 5975 (1977).

[54]I. P. Batra, S. Ciraci, and W. E. Rudge, Phys. Rev. B **15**, 5858 (1977).

[55]I. P. Batra, Phys. Rev. B **17**, 4114 (1978).

[56]L. Mihich, Solid State Commun. **28**, 521 (1978).

[57]A. Oshiyama and H. Kamimura, J. Phys. C **14**, 5091 (1981).

[58]L. Ley, Phys. Rev. Lett. **35**, 1796 (1975).

[59]P. Mengel, P. M. Grant, W. E. Rudge, B. H. Schechtman, and D. W. Rice, Phys. Rev. Lett. **35**, 1803 (1975).

[60]E. E. Koch and W. D. Grobman, Solid State Commun. **23**, 49 (1977).
[61]J. Bordas, A. J. Grant, H. P. Hughes, A. Jakobsson, H. Kamimura, F. A. Levy, K. Nakao, Y. Natsume, and A. D. Yoffe, J. Phys. C **9**, L277 (1976).
[62]T. Mitani, H. Mori, S. Suga, T. Koda, S. Shin, K. Inoue, I. Nakada, and H. Kanzaki, J. Phys. Soc. Jpn. **47**, 679 (1979).
[63]T. Mitani, S. Suga, Y. Tokura, K. Koyama, I. Nakada, and T. Koda, Int. J. Quantum Chem. **18**, 655 (1980).
[64]T. Mitani, K. Koyama, H. Mori, T. Koda, and I. Nakada, J. Phys. Soc. Jpn. **51**, 3197 (1982).
[65]H. J. Stolz, E. Petri, and A. Otto, Phys. Status Solidi B **80**, 289 (1977).
[66]J. M. E. Harper, R. L. Greene, P. M. Grant, and G. B. Street, Phys. Rev. B **15**, 539 (1977).
[67]A. A. Bright, M. J. Cohen, A. F. Garito, A. J. Heeger, C. M. Mikulski, P. J. Russo, and A. G. MacDiarmid, Phys. Rev. Lett. **34**, 206 (1975).
[68]P. M. Grant, R. L Greene, and G. B. Street, Phys. Rev. Lett. **35**, 1743 (1975).
[69]A. I. Gutman, L. S. Agroskin, G. V. Papayan, L. P. Rautian, and O. S. Schachnina, Solid State Commun. **49**, 187 (1984).
[70]C. L. Lawson and R. J. Hanson, *Solving Least Squares Problems* (Prentice-Hall, Englewood Cliffs, NJ, 1974).
[71]H. Wendel, J. Phys. C **10**, 497 (1977).
[72]H. Temkin and D. B. Fitchen, Solid State Commun. **19**, 1181 (1976).
[73]H. Temkin and G. B. Street, Solid State Commun. **25**, 455 (1978).
[74]J. W. Macklin, G. B. Street, and W. D. Gill, J. Chem. Phys. **70**, 2425 (1979).
[75]K. J. Chang and M. L. Cohen, Phys. Rev. B **34**, 4552 (1986).
[76]P. K. Lam, M. M. Dacorogna, and M. L. Cohen, Phys. Rev. B **34**, 5065 (1986).
[77]M. Aoki, N. Suzuki, and K. Motizuki, J. Phys. Soc. Jpn. **56**, 3253 (1987).